International Journal of Thermal Sciences 49 (2010) 356–364

Contents lists available at ScienceDirect

International Journal of Thermal Sciences

journal homepage: www.elsevier.com/locate/ijts

Mass transfer correlation development for the presence of entry region coil as swirl promoter in tube

Vaka Murali Mohan [a,*], C. Srinivasa Kumar [c], V. Sujatha [b], P. Rajendra Prasad [b], S. Sarveswarao [b]

[a] TRR College of Engineering, Patancheru, Hyderabad, India
[b] Department of Chemical Engineering, Andhra University, Visakhapatnam – 03, A P., India
[c] Gopal Reddy College of Engineering and Technology, Patancheru, Hyderabad, India

ARTICLE INFO

Article history:
Received 23 November 2007
Received in revised form
10 March 2009
Accepted 24 June 2009
Available online 9 September 2009

Keywords:
Entry region coil
Insert promoter
Mass transfer
Swirl flow
Modeling
Tube

ABSTRACT

Model development for mass transfer correlation in the presence of entry region coil as swirl promoter in tubes was presented in this paper. Coils were tested within a geometrical pitch 0.015, 0.025, 0.035 m and coil length 0.065, 0.095, 0.125 m. The electrolyte was equimolal Potassium ferricyanide, Potassium ferrocyanide and excess sodium hydroxide. The mass transfer correlation is based on law of the wall similarity. A model was developed in terms of geometric parameters and presented.

$$\overline{g} = 3.14 \times 10^{8} \left[\mathrm{Re}_m^{+}\right]^{-0.006} \left(\frac{P_c}{D}\right)^{-0.17} \left(\frac{L_c}{D}\right)^{-3.04} \left(\frac{L_c}{c_l}\right)^{3.06}$$

1. Introduction

In recent years the process industries aim at the maximum out put with reduced equipment size so as to minimize the unit product cost. This is particularly true in the design of electrolytic cells where the mass transfer limiting conditions exist. Various techniques have been adopted to augment the transfer rates. Use of turbulence promoter is one such technique that increases the transfer coefficients by several folds over the flow through smooth tube. Lin et al. [1] presented a theoretical analysis of mass transfer between a turbulent fluid stream and the wall.

The application of surface promoters, swirl generators, insert promoters, tubes of different geometric shapes increase the mass transfer coefficients at the reaction surface significantly by generating turbulence in the flow. Vibration of the reaction surface, pulsation, rotation of fluid, application of two phase flow, or three phase flow, magnetic and electric fields were few other techniques generally employed to obtain enhanced transfer rates. Among the above, insert promoters were employed with advantages of easy fabrication, operations and maintenance. Efforts are also made towards the use of combination of the different types of promoters. Incase of insert promoters the flow fields vary with the shape of the promoter and are generally complex. In such cases, experimental data can be analyzed in terms of dimensionless geometric groups of the promoter.

Several investigations were made earlier using coils as swirl generating turbulence promoter. Chiou [2] made experimental investigation for the augmentation of heat transfer coefficient in forced convection heat transfer. He employed spiral spring coil as an insert promoter in circular tube. Changal Raju [3] obtained data for mass transfer at wall electrodes using limiting current technique. Coils of different sizes wound on central annular rod were used as promoter. Paisarn Naphon [4,15] investigated the heat transfer characteristics and the pressure drop of the horizontal double pipe with coil-wire insert. Alberto Garcıa et al. [5] studied wire coil inserts offer their best performance within the transition region. Rajendra Prasad, P [6] studied ionic mass and momentum transfer with coaxially placed spiral coils as turbulent promoter in homogeneous flow and in fluidized beds and did experiments using ferro-ferri cyanide system by limiting current technique. Rahai and Wong [7] presented the experimental investigations of turbulent jets from round tubes with coil inserts. Kumar and Judd [8] studied the effect of coiled wire turbulence promoters in their heat and momentum transfer studies in single phase forced convection flow. Mass transfer with entry region coil as swirl promoter was selected for the present study.

* Corresponding author. Tel.: +91 9966023477; fax: +91 891 2747969.
E-mail address: murali_vaka@yahoo.com (V.M. Mohan).

1290-0729/$ – see front matter © 2009 Elsevier Masson SAS. All rights reserved.
doi:10.1016/j.ijthermalsci.2009.06.010

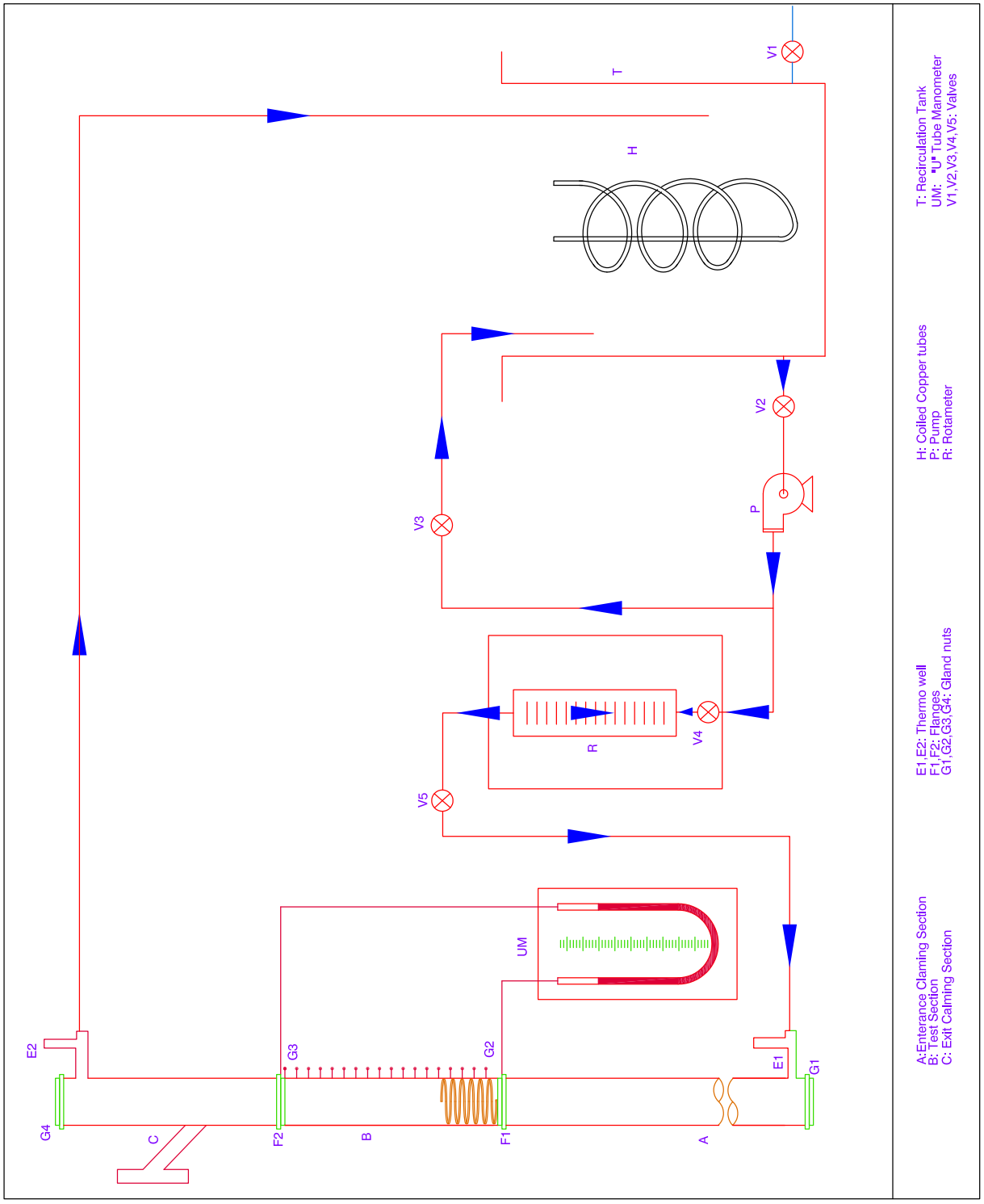

Fig. 1. Schematic diagram of experimental setup.

2. Experimentation

The schematic diagram of the experimental set up is shown in Fig. 1. The experimental set up essentially consisted of a re-circulating tank, a centrifugal pump, two rotameters, an entrance calming section, a test section, and an exit calming section was described by Rajendra Prasad [6]. The test section was provided with a number of point electrodes fixed flush with its surface longitudinally at equal spacing 0.03 m. The promoter was mounted in the test section coaxially by means of gland nuts and positioned by supporting grid. Spiral coil turbulence promoter was made of copper wire with provision to fix it rigidly within test section. The details of the entry region coil promoter were shown in Fig. 2. After inserting the promoter in the column, One-hundred liter of the electrolyte consisting of 0.01 M potassium ferricyanide, 0.01 M potassium ferrocyanide, and 0.5 N sodium hydroxide was prepared in the storage tank. The electrolyte is Newtonian and it has density of 1023 kg/m^3. Room temperature is around 30 °C. Temperature is recorded for every reading of the pressure drop using thermometer with 0.1 °C accuracy. This ensures the accuracy of physical properties such as μ, D, ρ. Thermometers are attached at both ends of the column. The electrolyte was pumped through the test section. The adjusting flow rates of the electrolyte by operating the control and by pass valves. Limiting current data were measured at point copper electrodes for the reduction of potassium ferricyanide ion and for the oxidation of potassium ferrocyanide ion. The electrochemical reactions involved are given below:

$$Fe[(CN)_6]^{-3} + e^- \rightarrow Fe[(CN)_6]^{-4} \text{ for reduction} \quad \text{(a)}$$

The limiting current was indicated by a small increase in current for a sharp increase in voltage. The experiments were repeated by varying the pitch of the coil (P_c) and Length of the coil (L_c). The information is highly useful in the design and development of energy efficient transfer operations. The range of variables covered is given in Table 1. Mass transfer coefficients are calculated by the following expression:

$$k_L = \frac{I_L}{nAFc_i} \quad \text{(b)}$$

3. Theory

The electrolyte through tubular flow reactor with entry region coil insert promoters will establish momentum and concentration profiles and was shown in Fig. 3. The profile is divided into two regions, the inner region and outer region. The inner region again divided into laminar sub layer and viscous–buffer zone. The outer region is turbulent core region and is fully turbulent. A model is developed with the following assumptions:

1. The fluid is Newtonian, incompressible, and has constant transport properties and independent of time.
2. Flow through smooth tube is fully developed with no entrance effects. The effect of body forces is small in comparison to that of viscous and inertial forces.
3. The axial velocity profile is independent of axial coordinate, similarly the concentration gradients.
4. The mass flux varies in the radial direction. The mass flux varies linearly with y, and is represented by

$$\frac{N}{N_w} = 1 - \frac{y}{R} \quad (1)$$

The radial variation of mass flux is taken into account by dividing into viscous–buffer zone and turbulent core. The flux at

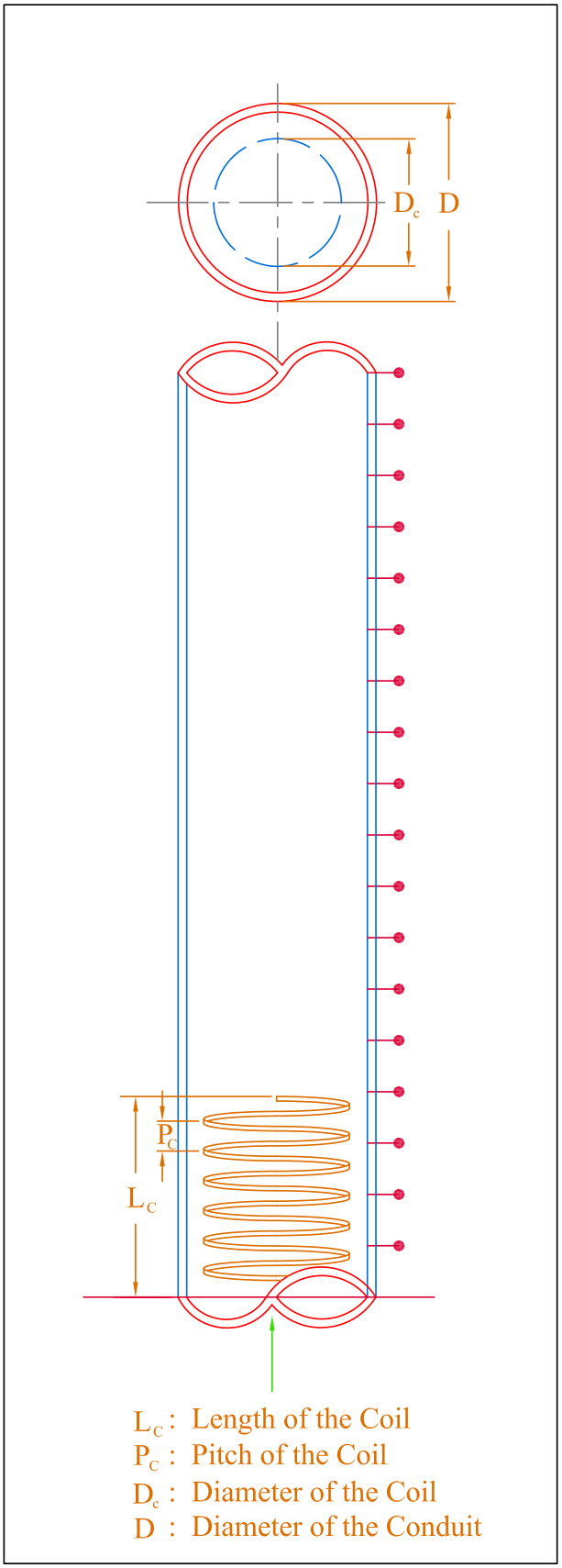

Fig. 2. Details of text section.

Table 1
Range of variables covered in the present study.

Variable	Minimum	Maximum
Pitch of the coil, m/turn	0.015	0.035
Length of the coil, m	0.035	0.125
Velocity, m/s	0.0591	0.2751

the interface is considered radially opposite directions, Flux at the interface towards the wall,

$$N_{i(v-b)} = k_{(v-b)}(c_i - 0) \tag{2}$$

Flux at the interface towards the axis,

$$N_{i(t)} = -k_{(t)}(c_i - c_b) \tag{3}$$

5. The shear stress is constant in the radial direction. Deissler and Eian [9] have found that the velocity and concentration profiles are relatively insensitive to shear stress distribution for fully developed turbulent fluid flow, hence can be assumed constant.
6. In the viscous–buffer zone, the eddy diffusivity and eddy viscosity ratio varies along with the distance from the wall and is independent of Sc. Direct numerical simulations presented by Lyons et al. [10] suggest Sc to be unity at the wall. Hence, in the present case it is assumed that as $y^+ \to 0$, $Sc = 1$.
7. The eddy diffusivity controls transfer process in viscous–buffer zone, while eddy viscosity controls the transport in turbulent core.

4. Model development

In turbulent core, the intensity of eddies will be higher than the v–b zone. Therefore, during the transfer process, the resistance to the exchange of mass between the bulk fluid and the solid surface is often confined to the viscous and buffer region. The total resistance

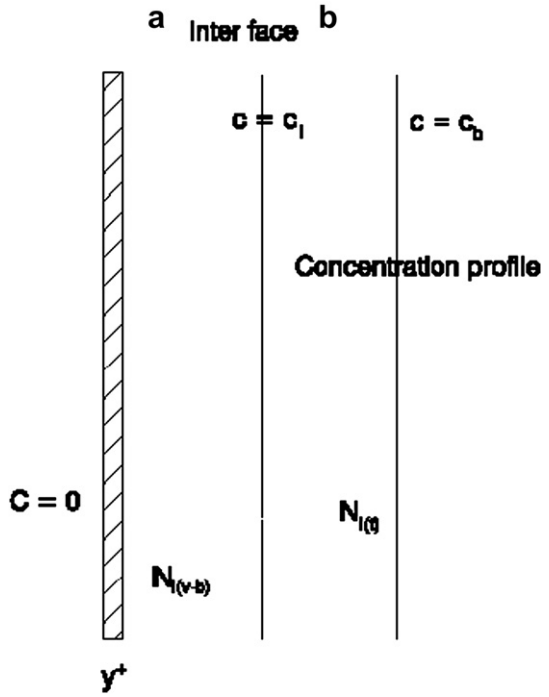

Fig. 3. Concentration changes in (a) Viscous–buffer zone and (b) turbulent core.

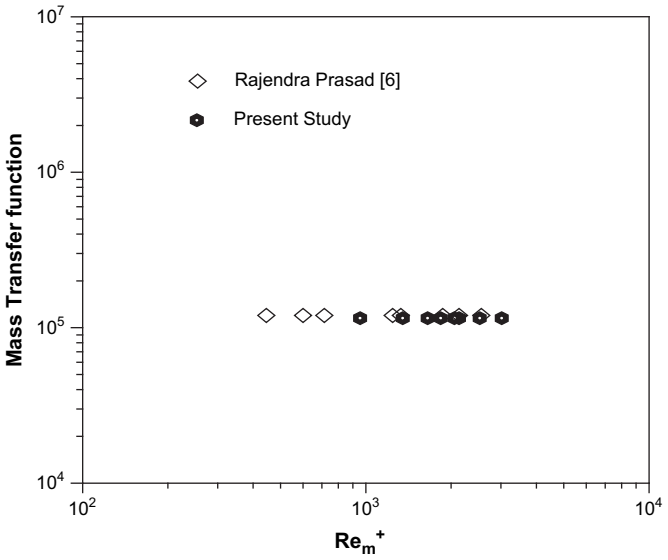

Fig. 4. Mass transfer correlation comparison – coil as promoter.

to the transfer process is the sum of the resistances in the viscous–buffer zone and turbulent layer proposed by Aravinth [11] and is represented by,

$$\frac{1}{k} = \frac{1}{k_{v-b}} + \frac{1}{k_t} \tag{4}$$

Eq. (4) represents a two-layer resistance separated by an interface, similar to that proposed by Hughmark [12]. The total resistance in the v–b zone and the turbulent core is represented by Eq. (4) and are similar to the boundary layer resistance and the resistance corresponding to random eddies in the region beyond the boundary layer. For a fully developed turbulent flow, the shear stress and the heat flux can be written as,

$$\tau = (\mu + \rho\varepsilon)\frac{du}{dy} = \rho(\nu + \varepsilon)\frac{du}{dy} \tag{5}$$

$$N = (D + D_e)\frac{dc}{dy} \tag{6}$$

4.1. In the viscous–buffer region

Equ. (6) on integration with the boundary conditions: at $y = 0$, $c = 0$ and at $y = y_i^+$, $c = c_i$

$$\frac{dc}{N_{i(v-b)}} = \int_0^{y_i} \frac{dy}{D + D_e}$$

Substitute Equ. (5) in (6)

$$\frac{\Delta c}{N_{i(v-b)}} = \frac{1}{\sqrt{\tau_0/\rho}} \int_0^{y_i^+} \frac{dy^+}{\frac{1}{Sc} + \frac{D_e(y^+)}{\upsilon}} \tag{7}$$

Combining Equ. (2) and (7) yields,

$$\frac{1}{k_{v-b}} = \frac{1}{\sqrt{\tau_0/\rho}} \int_0^{y_i^+} \frac{dy^+}{\frac{1}{Sc} + \frac{D_e(y^+)}{\upsilon}} \tag{8}$$

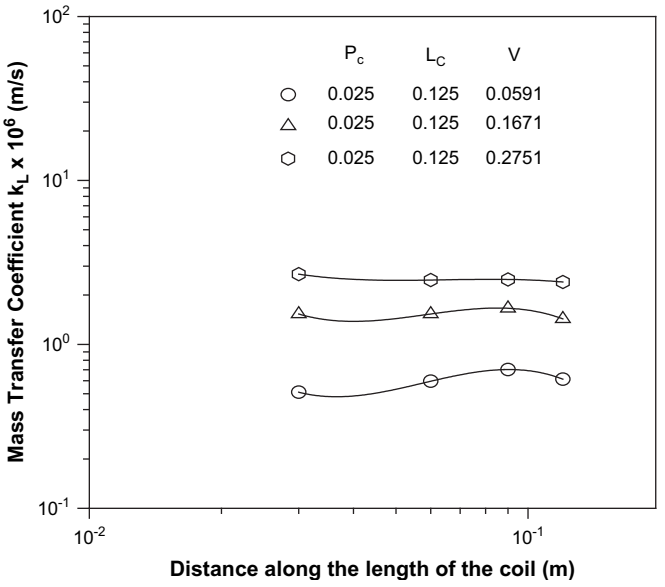

Fig. 5. Variation of k_L with distance along the length of the coil.

4.2. In the turbulent core

As the transport is mainly by eddy means, the molecular diffusivity and the viscosity can be neglected. Combining Equ. (5) and (6) and integrating along the turbulent layer with the boundary conditions: $c = c_b$ at $u = u_b$ and $c = c_i$ at $u = u_i$, yields,

$$\frac{dc}{du} = \frac{N_{i(t)}}{\tau_0/\rho}\left(\frac{\nu_e}{D_e}\right)_t \tag{9}$$

Substitute Equ. (3) in (9)

$$\frac{1}{k_t} = \int_0^{y_1} \frac{-du}{\tau_0/\rho}\left(\frac{\nu_e}{D_e}\right)_t = \frac{-(u_i - u_b)}{\tau_0/\rho}\cdot\Phi \tag{10}$$

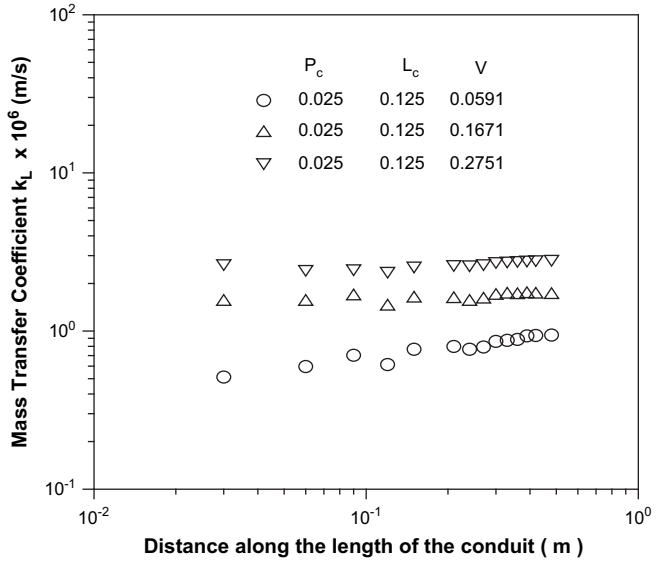

Fig. 6. Variation of k_L with distance along the length of the conduit.

$$\frac{1}{k_t} = \frac{\Phi u_b}{\tau_0/\rho}\left(1 - \frac{u_i/u^*}{u_b/u^*}\right) = \frac{\Phi u_b}{\tau_0/\rho}\left(1 - \frac{u_i^+}{u_b^+}\right) \tag{11}$$

In turbulent core $u_m \cong u_b$,

$$u_m^+ = u_b^+ = \sqrt{2/f} \tag{12}$$

Substitute Equ. (12) in (11)

$$\frac{1}{k_t} = \frac{\Phi u_b}{\tau_0/\rho}\left(1 - u_i^+\sqrt{f/2}\right) \tag{13}$$

Equ. (8) and (13) can be added using the resistance in series definition, i.e. Equ. (4)

$$\frac{1}{k} = \frac{1}{\sqrt{\tau_0/\rho}}\int_0^{y_1^+} \frac{dy^+}{\frac{1}{Sc} + \frac{D_e(y^+)}{\upsilon}} + \frac{\Phi u_b}{\tau_0/\rho}\left(1 - u_i^+\sqrt{f/2}\right) \tag{14}$$

Applying the assumption 7 that eddy viscosity controls the transfer process in turbulent core and the ratio $\Phi = 1$.

$$\frac{1}{k} = \int_0^{y_1^+} \frac{dy^+}{\frac{1}{Sc} + \frac{D_e(y^+)}{\upsilon}} + \sqrt{2/f} - u_i^+ \tag{15}$$

$$\frac{1}{k} = \frac{1}{St\cdot u_b} = \frac{1}{St\cdot\sqrt{2/f}} = \frac{\sqrt{f/2}}{St} \tag{16}$$

substitute Equ. (16) in (15).

$$\frac{f/2St - 1}{\sqrt{f/2}} + u_i^+ = \int_0^{y_1^+} \frac{dy^+}{\frac{1}{Sc} + \frac{D_e(y^+)}{\upsilon}} = g\left(Re_m^+, Sc\right)$$

$$\frac{f/2St - 1}{\sqrt{f/2}} + u_i^+ = g\left(Re_m^+, Sc\right) \tag{17}$$

The function g is written as product of $\bar{g}$ and $F(Sc)$.

$$g\left(Re_m^+, Sc\right) = \bar{g}\left(Re_m^+\right)F(Sc) \tag{18}$$

The law of wall can also represent well for the present study. Integral of Equ. (16) is only dependent on Sc only and is represented by $F(Sc)$. The $F(Sc)$ expression obtained in Prandtl and Von Karman anology is chosen for the present study. It is also supported by Deissler [13] and Sparrow and Malina [14] for $Sc > 1$ the empirical equation of $F(Sc)$ is

$$F(Sc) = 9.3(Sc - 1)Sc^{-1/4} \tag{19}$$

$$Re_m^+ = \frac{d_d}{d}\cdot Re\cdot\sqrt{\frac{f}{2}} \tag{20}$$

The function $\bar{g}$ is influenced by Re_m^+ and geometric parameters.

$$\bar{g}\left(Re_m^+, \Phi_1, \Phi_2, \Phi_3\right)$$

The resultant function can be represented as

$$\bar{g} = CRe_m^{+n_1}, \Phi_1^{n_2}, \Phi_2^{n_3}, \Phi_3^{n_3}$$

$\Phi_1 = P_c/D$, $\Phi_2 = L_c/D$, $\Phi_3 = L_c/c_l$

Data yielded the following equation for entry region coil–disc assembly as turbulence promoter.

$$\overline{g} = 3.14 \times 10^{8}\left[\mathrm{Re}_m^{+}\right]^{-0.006}\left(\frac{P_c}{D}\right)^{-0.17}\left(\frac{L_c}{D}\right)^{-3.04}\left(\frac{L_c}{c_l}\right)^{3.06} \quad (21)$$

Average deviation = 7.68, Standard deviation = 8.45
$r^2 = 0.9998$, Equ. (21) is compared with the data of Rajendra Prasad [6] and shown in Fig. 4. The figure reveals that the data of Rajendra Prasad is well fitted in this correlation.

S.no	Variable	Equations	Error
1	g	$\sqrt{e_g^2} = \sqrt{(0.01)^2}$	0.01
2	R_{em}	$\sqrt{\mathrm{Re}_m} = \sqrt{(0.0105)^2}$	0.0105
3	P_c/D	$\sqrt{e_{P_c}^2 + e_D^2} = \sqrt{(0.0067)^2 + (0.2)^2}$	0.2001
4	L_c/D	$\sqrt{e_{D_w}^2 + e_D^2} = \sqrt{(0.0316)^2 + (0.2)^2}$	0.2002
5	D_w/D	$\sqrt{e_{L_c}^2 + e_D^2} = \sqrt{(0.0167)^2 + (0.2)^2}$	0.20069
6	L_c/C_f	$\sqrt{e_{L_c}^2 + e_{C_f}^2} = \sqrt{(0.20069)^2 + (0.01667)^2}$	0.20129
1	P_C	$e = (\delta_{P_C}/P_C)$	0.0067
2	L_C	$e = (\delta_{L_C}/L_C)$	0.01667
3	D	$e = (\delta_D/D)$	0.2
4	C_f	$e = (\delta_{C_f}/C_f)$	0.0167
5	dw	$e = (\delta_{dw}/dw)$	0.0136
6	D_C	$e = (\delta_{D_C}/D_C)$	0.02
7	Q_C	$e = (\delta_{Q_C}/Q_C)$	0.1
8	ρ	$e = (\delta_\rho/\rho)$	0.1
9	g	$e = (\delta_Q/Q)$	0.01
10	Q	$e = (\delta_Q/Q)$	1
11	i_L	$e = (\delta_{i_L}/i_L)$	0.004
12	μ	$e = (\delta_\mu/\mu)$	0.1

4.3. Uncertainty analysis of experimental results

Calculation of error in Re:

$$\mathrm{Re} = \frac{DV\rho}{\mu}$$

Error in Re:

$$\mathrm{Re} = \sqrt{e_D^2 + e_V^2 + e_\rho^2 + e_\mu^2}$$
$$= \sqrt{(0.2)^2+(0.3)^2+(0.1)^2+(0.1)^2}$$
$$\mathrm{Re} = 0.387$$

Estimation Procedure for the calculation of error in V:

$$\mathbf{V} = \mathbf{Q}/\mathbf{A}$$
$$\mathbf{v} = \frac{Q}{\pi\frac{D^2}{4}} = \frac{Q}{A_f}$$

Error in V:

$$V = \sqrt{e_Q^2 + e_{Af}^2}$$
$$= \sqrt{(0.1)^2+(0.0004)^2}$$
$$V = 0.1000$$

$$\textbf{Calculation of error in Area of Electrode} = \frac{\left(0.01 \times 10^{-3}\right)}{\frac{\pi}{4}\left(0.0316 \times 10^{-2}\right)}$$
$$= 0.0402$$

Calculation of error in f:

$$f = \frac{\Delta P D g_c}{2V^2 C_f}$$

Error in the following parameters:

$\Delta P = 0.173$
$D = 0.2$
$g_C = 1$
$V^2 = 0.10012$
$C_f = 0.0167$

$$f = \sqrt{e_{\Delta P}^2 + e_D^2 + e_V^2 + e_{C_f}^2}$$
$$= \sqrt{(0.173)^2+(0.2)^2+(0.0167)^2+(0.1000)^2}$$
$$= 0.283$$

Calculation of ΔP:
Equation for the calculation of pressure drop
$\Delta P = \rho g h$

Variable	Error
ρ	0.1
g	0.01
h	0.1

Error in ΔP:

$$\Delta P = \sqrt{e_\rho^2 + e_g^2 + e_h^2}$$
$$= \sqrt{(0.1)^2+(0.1)^2+(0.01)^2}$$
$$= 0.1417$$

Calculation of error in Re_m^+:

$$\mathrm{Re}_m^+ = \frac{D_w}{D}\mathrm{Re}\sqrt{\frac{f}{2}}$$
$$= \frac{D_w}{D}\cdot\frac{DV\rho}{\mu}\cdot\frac{\Delta P D g_c}{2V^2 C_f \rho}$$

Error in Re_m^+:

$$\mathrm{Re}_m^+ = \sqrt{e_{D_w}^2 + e_V^2 + e_\rho^2 + e_\mu^2 + e_{\Delta_p}^2 + e_D^2 + e_{C_f}^2}$$
$$= \sqrt{(0.0316)^2+(0.3)^2+(0.1)^2+(0.1)^2+(0.173)^2+(0.2)^2+(0.0167)^2}$$
$$= 0.1812$$

Calculation of error in $\overline{g}$:

Equation for calculation of $\overline{g}$:

$$\overline{g} = \frac{\frac{f}{2}\mathrm{St} - 1}{\sqrt{\frac{f}{2}}} + R(h^+)$$

$$A_e = \frac{\pi D^2}{4} = \frac{\pi(0.316)^2}{4} = 0.0784$$

Error in A_e

$$A_e = \sqrt{e_{A_e}^2} = \sqrt{(0.0402)^2+(0.0402)^2} = 0.05685$$

Calculation of error in St:

$$\mathrm{St} = \frac{k_L}{V}$$

$$k_L = \frac{i_L}{A_e \cdot F \cdot C_o}$$

$$R(h^+) = \sqrt{e_{L_c/D}^2 + e_{P_c/D}^2 + e_f^2} = \sqrt{(0.0179)^2+(0.2001)^2+(0.283)^2} = 0.121$$

Error in C_o:

$$C_o = \sqrt{e_{\text{Weight of hypo}}^2 + e_{\text{volume}}^2}$$

$$W = \sqrt{(0.0403)^2+(0.001)^2} = 0.0403$$

Calculation of $\overline{g}$:

$$\overline{g} = \left(\frac{\frac{f}{2}\mathrm{St} - 1}{\sqrt{\frac{f}{2}}}\right) + R(h^+)$$

Error in $\overline{g}$:

$$\overline{g} = \sqrt{\left(e_{\overline{g}}^2\right) + \left(e_{R_{\mathrm{em}}^+}^2\right) + \left(e_{\frac{P_c}{D}}^2\right) + \left(e_{\frac{L_C}{D}}^2\right) + \left(e_{\frac{L_C}{C_f}}^2\right)}$$

$$= \sqrt{(1.886)^2 + \begin{pmatrix}(0.0327)^2\\+\\(0.0327)^2\\+\\(0.0327)^2\end{pmatrix} + \begin{pmatrix}(0.2001)^2\\+\\(0.2001)^2\\+\\(0.2001)^2\end{pmatrix} + \begin{pmatrix}(0.1738)^2\\+\\(0.1738)^2\\+\\(0.1738)^2\end{pmatrix} + \begin{pmatrix}(0.2013)^2\\+\\(0.2013)^2\\+\\(0.2013)^2\end{pmatrix}}$$

$$= 3.5866$$

$$e_{k_L} = \sqrt{(e^2 i_l) + \left(e_{A_e}^2\right) + \left(e_f^2\right) + \left(e_{C_o}^2\right)}$$

$$e_{k_L} = \sqrt{(0.004)^2+(0.05685)^2+(0.001)^2+(0.1)^2} = 0.1151$$

Error in St:

$$\mathrm{St} = \sqrt{(e^2 i_l) + \left(e_{A_e}^2\right) + \left(e_f^2\right) + \left(e_{C_o}^2\right)\left(e_V^2\right)}$$

$$\mathrm{St} = \sqrt{(0.004)^2+(0.0568)^2+(0.01)^2+(0.1)^2+(0.1000)^2} = 0.1525$$

Calculation of error in $R(h^+)$:

$$R(h^+) = 2.5\,Log\left(2x\frac{L_c/D}{P_c/D}\right) + \sqrt{\frac{2}{f}} + 3.75$$

Error in $R(h^+)$:

Model Equation:

$$\overline{g} = 3.14 \times 10^8 \left[\mathrm{Re}_m^+\right]^{-0.006} \left(\frac{P_c}{D}\right)^{-0.17} \left(\frac{L_C}{D}\right)^{-3.04} \left(\frac{L_c}{C_f}\right)^{3.06}$$

Error in model equation:

$$\overline{g} = \sqrt{\left(e_{\overline{g}}^2\right) + \left(e_{R_{\mathrm{em}}^+}^2\right) + \left(e_{\frac{P}{D_c}}^2\right) + \left(e_{\frac{L_C}{D}}^2\right) + \left(e_{\frac{L_C}{C_f}}^2\right)} = \sqrt{3.5866^2 + 0.1812^2 + 0.2001^2 + 0.2002^2 + 0.2013^2} = 3.608$$

5. Results

Entry region coil induced swirl flow in tube flow and continuous swirling along the length of tube; finally the flow reaches a smooth pipe flow. Because of induced swirl motion enhanced. The envisaged entry region swirl promoter have good potential in electro chemical reactors namely electro winning, refining, electro organic

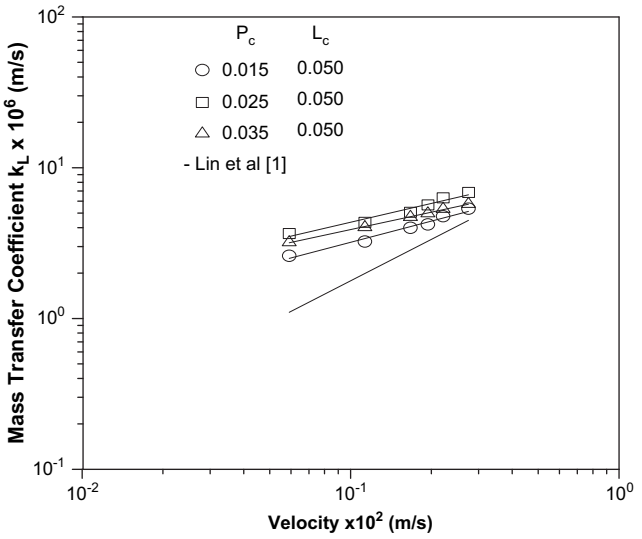

Fig. 7. Variation of k_L with velocity – pitch of the coil as parameter.

synthesis etc. Swirling of the source favors transition from laminar to turbulence as well as breakdown of coherent structures all around the fluid motion. A direct measurement method was applied in order to assess instantaneous entrainment coefficients, and results clearly show appreciable influence of the swirling motion on the flow development. Swirl flow devices form an important group of passive augmentation methods which entry region coil is one of the most important. Mass transfer coefficients are calculated by the equation (b). The local variation of mass transfer along the length of the coil and conduit and the effect of Pitch of the coil and length of the coil is discussed here under.

5.1. Local variation of mass transfer along the length of the coil

The data of mass transfer coefficient versus distance is plotted and shown in Fig. 5. The plots reveal mass transfer coefficient increased up to 0.1 m length of the coil and thereafter a decrease in coefficient is observed. As the velocity increased, the variation in mass transfer coefficient along the length of the coil is marginal.

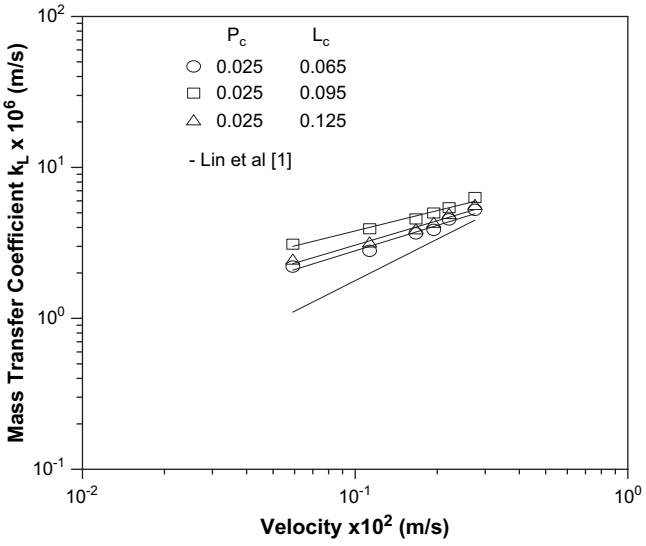

Fig. 8. Variation of k_L with velocity – length of the coil as parameter.

5.2. Local variation of mass transfer along the length of the tube

The variation of local mass transfer coefficients along the length of the tube for three different velocities are drawn and shown in Fig. 6. The figure shows that the mass transfer coefficients increased with velocity. The mass transfer coefficient values increased with the distance along the length of the conduit reached a maximum value, and there after i.e. beyond a certain length of the conduit, steady state flow conditions are attained and the k_L values remained constant. Further observations are necessary beyond the test section, to know the exact point at which it attains conduit flow with no promoter.

5.3. Effect of pitch of the coil

Pitch of the coil has a marked influence on fluid flow as it alters the axial flow while passing through the coil. To show the effect of pitch of the coil, k_L values are plotted against velocity for coils having different pitch values and the same coil lengths and are observed from Fig. 7. The plots reveal that mass transfer coefficient increased with increase in velocity. As the pitch of the coil increases the k_L values increase to maximum and further increase in pitch showed a decreasing trend. Similar observations were found by several researchers [2,3,5,6]. Augmentations achieved ranged from 2.27 to 3.18 fold at a velocity of 0.0591 m/s and that 1.19–1.60 fold at a velocity of 0.2751 m/s over Lin et al.

5.4. Effect of length of the coil

Coil length has a significant influence as it alters the axial flow of the fluid. The axial flow slowly transforms into swirl flow while the fluid passes along the length of the coil. The fluid leaving the coil has maximum swirl, and as it moves further the swirl decays, finally reaches to steady state, transforming again to an axial flow. All these changes in the flow enhances mass transfer coefficient by increasing the turbulence. Effect of length of the coil is clearly observed from Fig. 8. Mass transfer coefficient increases with increase in length of the coil upto a maximum, further increase in length shown a decreasing trend. Augmentations achieved are 1.91–2.73 fold at 0.0591 m/s and 1.07–1.36 fold at 0.2751 m/s over Lin et al.

6. Conclusions

Mass transfer coefficients increase with increase the velocity of the fluid and gives 3.18 fold augmentation over smooth tube flow. As the pitch of the coil increases the k_L values increase to maximum and further increase in pitch showed a decreasing trend. Mass transfer coefficient increases with increase in length of the coil upto a maximum, further increase in length shown a decreasing trend. A model was developed in terms of geometric parameters and presented.

$$\overline{g} = 3.14 \times 10^8 \left[\mathrm{Re}_m^+\right]^{-0.006} \left(\frac{P_c}{D}\right)^{-0.17} \left(\frac{L_c}{D}\right)^{-3.04} \left(\frac{L_c}{c_l}\right)^{3.06}$$

References

[1] C.S. Lin, R.W. Moulton, G.L. Putnam, Mass transfer between solid wall and fluid streams, Ind. Eng. Chem. 45 (3) (1953) 636–640.
[2] J.P. Chiou, Experimental investigation of the augmentation of forced convection heat transfer in a circular tube using spiral spring inserts, Trans. A.S.M.E. 109 (1987) 300–307.
[3] D. Changal Raju, Augmentation of mass transfer at the outer wall of concentric annuli in absence and presence of fluidizing solids effect of wires wound on central rod. Ph.D. thesis, Andhra University, Visakhapatnam, 1984.

[4] P. Naphon, Effect of coil wire insert on heat transfer enhancement and pressure drop of the horizontal concentric tubes, Int. Commun. Heat Mass Trans. 33 (2006) 753–763.
[5] A. García, P.G. Vicente, A. Viedma, Experimental study of H T enhancement with wire coil inserts in laminar transition turbulent regimes at different Prandtl numbers, Int. J. Heat Mass Trans. 48 (2005) 4640–4651.
[6] P. Rajendra Prasad, Studies on ionic mass transfer with coaxially placed spiral coils as turbulence promoter in homogenous flow and in fluidised beds. Ph.D thesis, Andhra University, India, 1993.
[7] P. Rajendra Prasad, V. Sujatha, C. Bhaskara Sarma, G.J.V.J. Raju, Studies on ionic mass transfer in the presence of spiral coil turbulence promoter in batch fluidised beds, Chem. Eng. Process. 43 (2004) 1055–1063.
[8] H.R. Rahai, T.W. Wong, Velocity field characteristics of turbulent jets from round tubes with coil inserts, Appl. Ther. Eng. 22 (9) (2002) 1037–1045.
[9] P. Kumar, R.L. Judd, Can. J. Chem. Eng. 48 (1967) 378–383.
[10] R.G. Deissler, C.S. Eian, Analytical and experimental investigation of adiabatic turbulent flow in smooth tubes, Nat. Adv. Commun. Aeronaut (1952) Washington, DC, TN-2629.
[11] S.L. Lyons, T.J. Hanratty, J.B. McLaughlin, Direct numerical simulations of passive heat transfer in turbulent channel flow, Int. J. Heat Mass Trans. 34 (1991) 1149–1156.
[12] S. Aravinth, Prediction of heat and mass transfer for fully developed turbulent flow through tubes, Int. J. Heat Mass Trans. 43 (2000) 1399–1408.
[13] G.A. Hughmark, Momentum, heat, and mass transfer analogy for turbulent flow in circular pipes, Ind. Eng. Chem. Fund. 8 (1969) 31–35.
[14] R.G. Deissler, Analysis of turbulent heat transfer, mass transfer and friction in smooth tubes at high Prandtl and Schmidt Washington, DC, TN, Nat. Adv. Comm. Aeronaut (1955) 1210.
[15] E.M. Sparrow, J.A. Malina, Variable property, constant-property, and entrance-region HT results for turbulent flow of water and oil in a circular tube, Chem. Eng. Sci. J. 19 (1964) 953–961.

List of symbols

A = Area of electrode, m^2
c = concentration of electrolyte, kg-mole/m^3
c_l = length of the conduit, m
D = diameter of the conduit, m
D_e = eddy diffusivity, m^2/s
F = faraday's constant = 96,500 C/g-mole
h_d = height of the disc, m
I_L = limiting current density, amps
k_L = mass transfer coefficient, m/s
L_c = Length of the coil, m
N = mass flux
P_c = Pitch of the coil, m/turn
R = radius of the conduit, m
u_i = velocity at the interface, m/s
u_b = average velocity, m/s
u^* = friction velocity, $\sqrt{\tau_0/\rho}$
u_i^+ = dimensionless velocity, u/u^*
u_b^+ = dimensionless bulk velocity
u_m^+ = average fluid velocity, m/s,
V = superficial velocity, m/s
y = coordinate distance normal to wall, m
$y_1 u_b$ = distance from wall at which $u =$
y_1^+ = dimensionless distance, yu^*/ν

Dimensionless
$\overline{g}$ = modified mass transfer function
Re_m^+ = modified Reynolds number
St = Stanton number, k/u_b or k_L/ν
Sc = Schmidt number, ν/D
Φ = ratio between molecular viscosity and eddy viscosity, $(\nu_e/D_e)_t$
$\Phi_1 = P_c/D$
$\Phi_2 = L_c/D$
$\Phi_3 = L_c/c_l$
n = number of ions transferred

Greek symbols
τ = shear stress, kg/ms^2
μ = viscosity of the fluid, poise
ρ = density of the fluid, kg/m^3
τ_0 = wall shear stress, $kg/m\,s^2$, $f/2 \cdot \rho \cdot u_b^2$
υ = kinematics viscosity
υ_e = eddy kinematics viscosity

Subscripts
b = buffer
i = interface
t = turbulent
o = wall
v = viscous
v–b = viscous–buffer region